Magnetic nuclear spin-lattice relaxation in NMR of orthorhombic crystals in the presence of strong quadrupole coupling



1992 J. Phys.: Condens. Matter 4 5811

(http://iopscience.iop.org/0953-8984/4/26/015)

J. Phys.: Condens. Matter 4 (1992) 5811–5824. Printed in the UK

# Magnetic nuclear spin–lattice relaxation in NMR of orthorhombic crystals in the presence of strong quadrupole coupling

Mladen Horvatić

Institute of Physics of the University of Zagreb, Bijenička 46, PO Box 304, 41001 Zagreb, Croatia

Received 6 February 1992, in final form 20 March 1992

**Abstract.** A review is given of some NMR techniques developed in experiments on high-temperature superconductors. Multiexponential relaxation which appears in the $T_1$ measurements when NMR lines are split by quadrupole interactions is discussed for the case of magnetic relaxation. The change in the form of relaxation is followed as the quadrupole Hamiltonian starts to perturb the otherwise pure Zeeman spin states (defined by $I_z$). Orthorhombic symmetry is assumed in the analysis, which is shown to greatly simplify the data reduction to obtain the magnetic hyperfine shift, the electric field gradient and the nuclear spin–lattice relaxation rate.

## 1. Introduction

Nuclear spins larger than 1/2 have non-zero electric quadrupole moments which interact with the electric field gradient (EFG) if it is present at the position of the nucleus. By NMR one can measure the EFG tensor [1] and use it as important information about the system under investigation. However, the technique of the NMR data reduction to obtain the magnetic hyperfine shift (MHS) (which is called the Knight shift in metals), the EFG and the nuclear spin–lattice relaxation rate (NSLRR) can be considerably more difficult than in the case of spin 1/2 or zero EFG. Recent examples are given by a large number of NMR results on high-temperature superconductors (HTSC) [2] and notably in YBCO compound for copper $^{63,65}$Cu spin 3/2 nuclei [3–6] and oxygen $^{17}$O spin 5/2 nuclei [7–9]. Fortunately, in orthorhombic crystals, for NMR sites having local symmetry $mm2$, the principal axes of the MHS and EFG tensors have to be parallel to the crystal axes, which greatly simplifies the NMR measurements and data analysis. In this paper we focus on these 'technical details' (usually taken into account implicitly in most of the NMR publications) underlying the NMR work in orthorhombic compounds in the presence of strong quadrupole coupling to the EFG [10]. The central point is the detailed discussion (given in section 3) of the multiexponential relaxation in the NSLRR measurements, which has proved to be of prime importance in experimental work and can possibly lead to serious systematic errors. The basis of the analysis is the orthorhombic symmetry of the samples and the local symmetry $mm2$, and in section 2 we will also explore to some extent the simplifications and technical details based on this symmetry, which have been developed in the course of investigation of $^{63}$Cu and $^{17}$O NMR in HTSC.

0953-8984/92/265811+14$04.50  

## 2. Magnetic hyperfine shift and electric field gradient

Both the EFG and the MHS tensors are symmetric and in orthorhombic crystals one would naturally like to have the principal axes of these tensors simply parallel to the crystal axes. However, it turns out that, in general, the local symmetry at a particular NMR site in an orthorhombic crystal may not be high enough to ensure this parallelism automatically. One sufficient condition is the local symmetry $mm2$, i.e. it is enough to find at least two of the three crystal planes ($a$–$b$, $b$–$c$ and $c$–$a$) passing through the position of the nucleus to be the planes of mirror symmetry. By symmetry, for each of these two planes there is a principal axis that has to be perpendicular to the plane, which is enough to fix the coordinate system of principal axes parallel to the crystal axes. The given criterion is very simple and it is easy to verify that it is fulfilled e.g. for all the nuclei in YBCO HTSC. This is a fundamental simplification, as in general the number of unknown parameters is reduced by two times three Euler angles (which would otherwise be necessary to specify the position of the coordinate system of principal axes) corresponding to the MHS and EFG tensors. In this case, for the Hamiltonian $\mathcal{H}$ which determines the energy levels of nuclear spins and thus the positions of the NMR lines, we can simply use the coordinate system of crystal axes in which all tensors are diagonal:

$$\begin{aligned} \mathcal{H} &= \mathcal{H}_{\text{Zeeman}} + \mathcal{H}_{\text{Quadrupole}} \\ \mathcal{H}_{\text{Zeeman}} &= \sum_{A=a,b,c} -\hbar\gamma_n(1+K_{AA})H_{0_A}I_A \\ \mathcal{H}_{\text{Quadrupole}} &= h\nu_{zz}\left[3I_z^2 - I(I+1) + \eta_z(I_+^2 + I_-^2)/2\right]/6 \end{aligned} \tag{1}$$

where $\eta_z = (\nu_{xx} - \nu_{yy})/\nu_{zz}$, $x$, $y$, $z$ correspond to any combination of the $a$, $b$, $c$ axes with no restrictions, and otherwise standard notation [1] has been used. We recall here that frequencies $\nu_{AA}$ are proportional to the EFG $V_{AA}$ : $\nu_{AA} = 3eQ/[2hI(2I-1)]V_{AA}$ [1]. According to Poisson's equation, the EFG tensor has zero trace and in the quadrupole Hamiltonian it is therefore represented by only two parameters $\nu_{zz}$ and $\eta_z$.

Altogether, the Hamiltonian contains as many as five unknown parameters which fully determine the MHS and EFG tensors, and it is explicitly dependent on the orientation of the external magnetic field $\boldsymbol{H}_0$. The logical choice is to orient $\boldsymbol{H}_0$ parallel to one of the crystal axes and in the following we will take this axis to be $z$-axis, i.e. $\boldsymbol{H}_0 = H_0\boldsymbol{k}$. In the Hamiltonian (1) the Zeeman part is simplified,

$$\mathcal{H} = -\hbar\gamma_n(1+K_{zz})H_0I_z + h\nu_{zz}\left[3I_z^2 - I(I+1) + \eta_z(I_+^2 + I_-^2)/2\right]/6 \tag{2}$$

and only three parameters $K_{zz}$, $\nu_{zz}$ and $\eta_z$ are left over. These can be determined from only three lines of the corresponding NMR spectrum so only one complete spectrum (i.e. for one orientation of the sample) for spin $\geqslant 3/2$ is required to provide the complete EFG tensor (plus one component of MHS). This fact proved to be fundamental in the NMR investigation of $YBa_2Cu_3O_7$ HTSC, where the symmetry of the EFG tensor has been used as the decisive argument to solve the long-lasting controversy in the site assignment of two copper lines [3, 4]. Although the symmetry of the MHS tensor can be used for the same purpose, in principle we need measurements

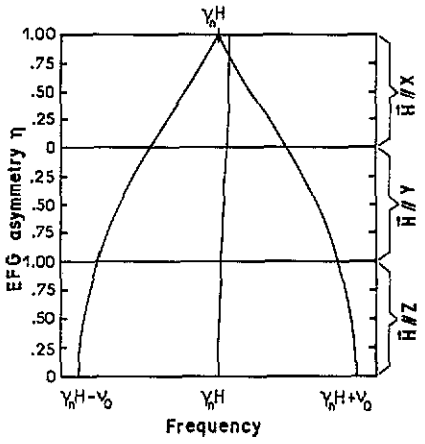


**Figure 1.** Line positions as a function of the asymmetry parameter in the NMR of a spin $I = 3/2$, in the presence of strong quadrupole coupling, when $H_0$ is applied parallel to any of the principal axes of the EFG tensor.

for three different orientations of the sample for its determination while the use of EFG is much simpler as only one spectrum is needed.

Figure 1 shows an example (corresponding to copper resonance in copper-oxide HTSC) where the line positions of spin 3/2 are obtained from the exact solution of Hamiltonian (1) for $H_0$ parallel to any of the principal axes $X$, $Y$ and $Z$†. In order to emphasize the dependence of the line positions on the symmetry of the EFG tensor, in figure 1 the MHS has been absorbed in the 'total' magnetic field, $H = (1 + K_{AA})H_0$. The NQR frequency $\nu_{NQR} = \nu_{ZZ}(1 + \eta_Z^2/3)^{1/2}$ has been kept constant, which corresponds to the actual experimental situation with copper NMR in $YBa_2Cu_3O_7$, where this parameter had been known from pure NQR before the determination of the complete EFG tensor. Using the symmetry properties of the Hamiltonian (1) under the exchange of the principal axes, it can be shown that in the representation of figure 1 the line positions (as a function of $\eta$ and orientation) are given by continuous smooth lines, regardless of the spin value. For $H_0$ parallel to the $Z$-axis and $\eta = 0$, the NMR lines are equally spaced out at intervals equal to $\nu_Q$ and with the central line [for half-integer spins, transition (1/2, −1/2)] at exactly $\gamma_n H/2\pi$, i.e. *not* shifted by the quadrupole coupling. For all other cases, as we move upwards along the vertical axis of figure 1, the intervals between the lines decrease monotonically and they are no longer equal; the higher-frequency interval is somewhat smaller than its lower-frequency neighbour. The central line is shifted by the quadrupole coupling to a higher frequency. From such dependence it is evident that the EFG parameters are uniquely determined by the line positions. To be more precise, one can determine $\nu_{zz}$ (up to its sign) and $\eta_z$, and from these calculate $\nu_{xx}$ and $\nu_{yy}$. However, for two crystal axes perpendicular to the $z$-axis one cannot tell which one is $x$- and which one is $y$-axis.

In the following we discuss in more detail our choice of $H_0$ as being parallel to one of the crystal axes, which underlies our analysis of the NMR spectrum. Experimentally there are two possible ways to ensure this condition: one is to take a single crystal and orient it appropriately; e.g. copper oxide HTSC single crystals are platelets with the $c$-axis perpendicular to the platelet. Another possibility is to make a so-called

† The convention $|\nu_{ZZ}| < |\nu_{YY}| < |\nu_{ZZ}| = \nu_Q$ restricting $\eta_Z = \eta$ to the interval $0 < \eta < 1$ is customary, but not necessary. When this convention is assumed we will use capital letters $X$, $Y$ and $Z$.

'oriented powder' where all grains in the powder are small single crystals oriented with e.g. their $c$-axes parallel to the external field, while the orientation of two perpendicular axes $a$ and $b$ is random. It turns out that for most HTSC the anisotropy of magnetic susceptibility at $T > T_c$ favours alignment of the $c$-axis parallel to the external magnetic field and it is relatively easy to perform the orientation *in situ* in the $H_0$ field. For $H_0$ parallel to the oriented axis (which is automatically obtained by orientation *in situ*), the same Hamiltonian describes each grain and the whole sample is indistinguishable from a true single crystal, as far as the NMR is concerned. The resulting spectrum consists of lines, and according to the previous discussion it is sufficient for the full determination of the EFG.

Note that as soon as we put $H_0$ perpendicular to the oriented axis of an oriented powder (which we can call a 'two-dimensional powder'), or in the case of non-oriented ('three dimensional') powder, the spectrum will correspond to the directional average over all possible directions of $H_0$ with respect to the crystal axes of each grain in the sample. Instead of lines, one obtains the distribution, and instead of line positions, in the determination of parameters one has to refer to 'van Hove' singularities in the spectrum. In this case the determination of parameters (if possible at all) is more difficult and less reliable. It is clear that the 'two-dimensional' (oriented) powder is preferred to the 'three-dimensional' powder as, due to lower dimension, van Hove singularities are sharper and the number of parameters describing the spectrum is smaller.

## 3. Nuclear spin–lattice relaxation

The theory of the multiexponential relaxation of spin $I > 1/2$ induced by the presence of quadrupole coupling was treated previously by Andrew and Tunstall [11] and Narath [12]. In recent measurements of copper and oxygen NSLRR in HTSC, this theory has been applied to obtain the explicit expressions for the relaxation of different lines of spin 3/2 and 5/2 spectra [4, 8]. These expressions correspond to relaxation of magnetic origin in the case when Zeeman spin states (i.e. the eigenstates of $I_z$) are only negligibly perturbed by the quadrupole coupling. The latter condition is fulfilled when the asymmetry of the quadrupole coupling with respect to the direction of magnetic field ($z$-axis) is much smaller than the Zeeman interaction:

$$h\nu_{zz}\eta_z \ll \hbar\gamma_n H_0. \tag{3}$$

Condition (3) ensures that the off-diagonal elements in Hamiltonian (2) be much smaller than the diagonal ones. Trivially, this can be ensured when the quadrupole coupling $\nu_{zz}$ is small, which is, e.g. the case of $^{17}O$ NMR in HTSC. This can also be true for strong quadrupole coupling and for the direction of the symmetry axis of the EFG tensor (for $\eta_z \ll 1$), which is just the case of copper in $CuO_2$ planes of HTSC, when $H_0$ is parallel to the $c$-axis. For the same nucleus and $H_0$ perpendicular to the $c$-axis, condition (3) is not fulfilled and more complicated analysis is needed in the determination of the relaxation rate. An analysis of this type appeared only very recently in connection with the low-field copper NMR [6], however, even in the high-field NMR these effects cannot be neglected. Similar analysis has also been given by Chepin and Ross [13] in the general treatment of pure NQR, i.e. in the case of zero

magnetic field. In the following, together with the most general treatment of multi-exponential relaxation, we present a detailed discussion of conditions corresponding to each type of fit, and cover all the cases from high to low magnetic field.

For the sake of completeness and generality, in appendix A we give the explicit expression for the time development of the energy level populations $n_i$, given the arbitrary probability of transition $W_{ij}$ from level $j$ to level $i$, and arbitrary initial conditions. The assumption underlying this approach is that the spin–spin interactions ensure that the population of energy levels of each nuclear spin can be treated statistically and described by the linear rate equation. Note that the solution of the linear rate equation given in appendix A is quite general regardless of the origin and size of the transition probabilities. The only NMR-specific detail in this solution is the standard choice of the variable [11, 12] which is taken to be the difference of populations of neighbouring energy levels $\Delta n_i = n_i - n_{i+1}$, as this quantity is directly proportional to the NMR signal. The transformation to the $\Delta n_i$ variables is given in matrix notation [14]—which is a great advantage, enabling direct and simple conversion of the procedure into a computer program capable of handling any particular case. Note that in [6, 13] the transformation has been avoided and the rate equation solved directly, leading to the appearance of a redundant eigenvector in the solution.

As the next step we discuss the initial condition corresponding to a particular experimental procedure. We consider the standard $\pi$–$t$–$\pi/2$–$\tau$–$\pi$ pulse sequence for the NSLRR measurements, where the excitation is performed by one short pulse at $t = 0$, exciting e.g. the $(m+1, m)$ line. This pulse is supposed to be the only source of variation of $[\Delta n_k(t=0) - \Delta n_k(t=\infty)]$, i.e. it has to be short enough for the relaxation during the pulse to be negligible. (Note that this might not be true for the excitation by a pulse sequence.) The spectral width of the excitation pulse has to be wide enough to cover the line completely, but also narrow enough to avoid 'touching' neighbouring lines. Under these conditions one has a well defined initial condition:

$$[n_k(0) - n_k(\infty)] \propto \tfrac{1}{2}(\delta_{k,m} - \delta_{k,m+1})$$

i.e.

$$[\Delta n_k(0) - \Delta n_k(\infty)] \propto \delta_{k,m} - \tfrac{1}{2}(\delta_{k,m+1} + \delta_{k,m-1}) \tag{4}$$

where $\delta_{km}$ is the Kronecker delta (i.e. $\delta_{km} = 0$ for $k \neq m$ and $\delta_{km} = 1$ for $k = m$). Note that a similar expression can also cover the case in which the NMR line corresponds to a transition between *any* two levels, and not only neighbouring ones.

The final fundamental ingredient which remains to be specified in our description of relaxation is of course the transition probability $W_{ij}$. We recall that from the first-order perturbation for the equation of motion of the density matrix [1], the probability of transition between localized energy levels $|k\rangle \rightarrow |m\rangle$, for a perturbation that is spread in frequency, is given by the $\omega_{mk}$ $[\omega_{mk} = (E_m - E_k)/\hbar]$ Fourier component of the interaction Hamiltonian correlation function:

$$W_{mk} = \hbar^{-2} \int_{-\infty}^{+\infty} \mathrm{d}t \, \exp(\mathrm{i}\omega_{mk} t) \overline{\langle m|\mathcal{H}_1(t)|k\rangle \langle k|\mathcal{H}_1(0)|m\rangle}. \tag{5}$$

In this paper we discuss only the relaxation of 'magnetic origin', i.e. the interaction Hamiltonian to be inserted in (5) is

$$\mathcal{H}_1 = -\hbar\gamma_n \boldsymbol{I}\cdot\boldsymbol{h}(t) \tag{6}$$

where $\boldsymbol{h}(t)$ is the fluctuating part of the local magnetic field (with zero time average). From (5, 6) it is clear that

$$u_{AB}(\omega) = \gamma_n^2 \int_{-\infty}^{+\infty} \mathrm{d}t\, \mathrm{e}^{\mathrm{i}\omega t}\overline{h_A(t)h_B(0)} \qquad A, B = x, y, z, +, - \tag{7}$$

will be the fundamental quantities in the transition probabilities. As a reference, we start with the spin 1/2 case with a single transition and no quadrupole coupling. Even in this case we can apply the procedure of appendix A to obtain single-exponential relaxation with time constant $T_1$ given by

$$T_1^{-1} = W_{1/2,-1/2} + W_{-1/2,1/2}. \tag{8}$$

From (5–8),

$$\begin{aligned} T_1^{-1}(\omega_0) &= u_{-+}(-\omega_0) + u_{+-}(\omega_0) \\ &= \tfrac{1}{2}\{[u_{xx}(\omega_0) + u_{yy}(\omega_0)] - \mathrm{i}[u_{xy}(\omega_0) - u_{yx}(\omega_0)]\} \end{aligned} \tag{9}$$

where $\omega_0$ is the NMR resonance frequency. (Note some relevant symmetry properties of the correlation function (7): for $A, B = x, y, z$, $u_{AB} - u_{BA}$ is imaginary and odd, while $u_{AA}$ and $u_{AB} + u_{BA}$ are real and even functions of $\omega$.) As the next step we consider the arbitrary spin in the presence of a weak quadrupole coupling which leaves the Zeeman spin states (almost) unperturbed. In this case only $I_+I_-$ and $I_-I_+$ combinations will provide non-zero contribution in the transition probabilities,

$$W_{mk} = \tfrac{1}{2}T_1^{-1}(\omega_{mk})[|\langle m|I^+|k\rangle|^2 + |\langle m|I^-|k\rangle|^2] \tag{10}$$

where $T_1^{-1}(\omega)$ is defined by (9). For weak quadrupole coupling, all transition frequencies are rather close, so that we can neglect the frequency dependence of $T_1$,

$$T_1^{-1}(\omega_{mk}) \cong T_1^{-1}(\omega_0) \tag{11}$$

and in the transition probabilities (10) only one parameter (namely $T_1$) is left over—the same as defined in the 'reference' spin 1/2 case. Using (10), (11) and the initial condition (4) in the procedure given in appendix A, it is a simple matter to obtain the time dependence in the relaxation experiment for an arbitrary spin. The spin 3/2 and 5/2 curves obtained in this way (which are much used in the investigation of $^{63}$Cu and $^{17}$O NMR in HTSC) are given in table 1. Figure 2 shows an example of the fit to the spin 5/2 curve, corresponding to the relaxation of plane oxygen in YBCO HTSC [9]. Note that the same analysis and the same curves are valid even for strong coupling with only weak asymmetry (3), under the condition that $T_1^{-1}(\omega)$ is frequency-independent in the frequency range where the NMR lines are observed. An example is provided by the relaxation of plane copper in YBCO, when $\boldsymbol{H}_0$ is parallel to the $c$-axis. Frequency independence of $u_{AB}(\omega)$ correlation functions (7) is actually

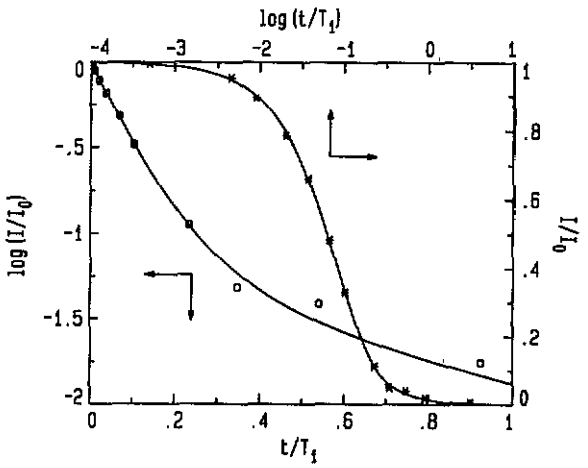


**Figure 2.** Theoretical fit (table 1) and the relaxation data used for the determination of $T_1$ of the plane oxygen in YBCO, measured on (3/2, 1/2) low-frequency satellite in the $H_0 \parallel X$-axis configuration, at 100 K [9]. The same data are shown in the standard linear–log plot and in the experimentally more appropriate log–linear plot.

expected to be fulfilled in most cases, as the correlation times of the magnetic field fluctuations are very short on the time scale defined by the NMR frequency (p 194 of [1]). Note that here we speak of the frequency independence of $T_1$ for given external magnetic field $H_0$, but at the same time $T_1$ may very well depend on $H_0$ reflecting the influence of magnetic field on the system; the two variables, i.e. magnetic field and frequency, have here different meanings which must not be confused.

So far, we have only repeated the analysis of Andrew and Tunstall [11] and Narath [12] in a way appropriate for the extension to the most general case. Now, if the Zeeman states are significantly mixed by the asymmetry of quadrupole coupling, in principle all the combinations $I_A I_B$ will appear when the interaction Hamiltonian (6) is inserted in the expression for the transition probability (5). To simplify the expression, we consider only the case where $H_0$ is parallel to one of the principal axes. Hamiltonian (2) can then be used for the description, and the only off-diagonal elements in the Hamiltonian are generated by $I_+^2$ and $I_-^2$ operators. Consequently, only Zeeman states with $\Delta M = \pm 2$ will be mixed together. (We also remark that in this case the Hamiltonian (2) and therefore all the spin states and all relevant matrix elements are real, which simplifies numerical treatment.) It is easy to see that in the transition probability only the $I_z I_\pm$ or $I_\pm I_z$ combinations give zero contribution and the complete expression is given by:

$$\begin{aligned} W_{mk} = {} & \tfrac{1}{2}\{[u_{xx} + u_{yy}] + \mathrm{i}[u_{xy} - u_{yx}]\}\,\tfrac{1}{2}\langle m|I_+|k\rangle^2 \\ & + \tfrac{1}{2}\{[u_{xx} + u_{yy}] - \mathrm{i}[u_{xy} - u_{yx}]\}\,\tfrac{1}{2}\langle m|I_-|k\rangle^2 \\ & + \tfrac{1}{2}[u_{xx} - u_{yy}]\langle m|I_+|k\rangle\langle k|I_+|m\rangle + u_{zz}\langle m|I_z|k\rangle^2 \end{aligned} \tag{12}$$

where all the correlation functions $u_{AB}$ are to be taken at the frequency of the transition $\omega = \omega_{mk}$, states $|m\rangle$ and $|k\rangle$ now refer to real spin states obtained from the solution of the Hamiltonian (2) and the matrix elements are explicitly taken to be real. In the discussion of this result we will suppose that the cross-correlation term

$[u_{xy} - u_{yx}]$ is zero (p 207 of [1]) and that all the correlation functions are frequency independent. This will reduce the number of parameters appearing in (12) to three ($u_{xx}$, $u_{yy}$ and $u_{zz}$), which can be converted to the above discussed relaxation rates (9) measured in the three directions of the principal axes, i.e.

$$W_{mk} = T_1(z)^{-1}\left[\tfrac{1}{2}(\langle m|I_+|k\rangle^2 + \langle m|I_-|k\rangle^2) + \{[T_1(y)^{-1} - T_1(x)^{-1}]/T_1(z)^{-1}\}\langle m|I_+|k\rangle\langle k|I_+|m\rangle + \{[T_1(y)^{-1} + T_1(x)^{-1}]/T_1(z)^{-1} - 1\}\langle m|I_z|k\rangle^2\right]. \quad (13)$$

Formally, (13) puts us in a rather unfavourable situation where the complete relaxation rate tensor has to be known in advance in order to find out the exact form of the relaxation curve necessary for its determination. The only way out is the iterative self-consistent determination of $T_1(x, y, z)$. Comparing (13) to (10) we notice that the new terms are linear ($I_+ I_+$) or quadratic ($I_z I_z$) in the quadrupole perturbation (or of a higher order). In the first approximation we can therefore rely on the above discussed case of pure Zeeman states and the known 'standard' relaxation curves (see table 1) to provide the first estimate of the anisotropies $T_1(x, y)^{-1}/T_1(z)^{-1}$ which are needed in expression (13). We then start an iterative procedure where previously approximated values of $T_1$ are used in the part of expression (13) in braces in order to define new transition probabilities and new relaxation curves which are then used to obtain the subsequent approximation of $T_1$—until the values converge.

**Table 1.** Magnetic relaxation in $T_1$ measurements, when quadrupole coupling splits the NMR lines but leaves the Zeeman spin states (almost) unperturbed.

| Spin | Transition | $F(x) = F(t/T_1)$; $F(0) = 1$ |
|---|---|---|
| 5/2 | $(-1/2, +1/2)$ | $\frac{1}{35}e^{-x} + \frac{8}{45}e^{-6x} + \frac{50}{63}e^{-15x}$ |
| | $(\mp 3/2, \mp 1/2)$ | $\frac{1}{35}e^{-x} + \frac{3}{56}e^{-3x} + \frac{1}{40}e^{-6x} + \frac{25}{56}e^{-10x} + \frac{25}{56}e^{-15x}$ |
| | $(\mp 5/2, \mp 3/2)$ | $\frac{1}{35}e^{-x} + \frac{3}{14}e^{-3x} + \frac{2}{5}e^{-6x} + \frac{2}{7}e^{-10x} + \frac{1}{14}e^{-15x}$ |
| 3/2 | $(-1/2, +1/2)$ | $\frac{1}{10}e^{-x} + \frac{9}{10}e^{-6x}$ |
| | $(\mp 3/2, \mp 1/2)$ | $\frac{1}{10}e^{-x} + \frac{5}{10}e^{-3x} + \frac{4}{10}e^{-6x}$ |

In the following, as an example, we discuss the results of Cu resonance in $CuO_2$ planes of YBCO HTSC. The situation is considerably simpler here because of the tetragonal symmetry. This means that for $H_0 \parallel c$-axis the simpler analysis based on (10) and the curves for spin 3/2 given in table 1 are valid exactly, provided that $T_1$ is not frequency dependent. The general analysis applies only to the determination of $T_1(a) = T_1(b)$, i.e. to the determination of the NSLRR anisotropy $R = T_1(a, b)^{-1}/T_1(c)^{-1}$. For the $a$ or $b$ direction, the parameters in the Hamiltonian (2) are $\nu_z = -\nu_Q/2$ and $\eta_z = \pm 3$, and the corresponding transition probabilities are given by

$$W_{mk} = T_1(a, b)^{-1}\left\{\tfrac{1}{2}(\langle m|I_+|k\rangle^2 + \langle m|I_-|k\rangle^2) \pm (1/R - 1)\langle m|I_+|k\rangle\langle k|I_+|m\rangle + (1/R)\langle m|I_z|k\rangle^2\right\}. \quad (14)$$

This expression has been used to show how the relaxation curve is modified by the quadrupole perturbation of spin states; in table 2 the explicit expressions are given

which correspond to the transition (3/2, 1/2) of plane copper in $YBa_2Cu_3O_7$ and various values of the magnetic field used in the investigations [5, 6, 9]. It is obvious that for $\gamma H_0 \lesssim \nu_Q$ one obtains substantial changes in the relaxation curve, and even at high fields, $\gamma H_0 \gg \nu_Q$, this effect cannot be neglected. To get a feeling how the deviation develops as we lower the magnetic field, one can compare the true relaxation curve and the 'standard curve' (i.e. the one corresponding to $H_0 \to \infty$) which is time scaled in order to minimize the difference between these two curves. In this case the time scaling factor will measure the error due to using the standard curve instead of the real one. An example of these corrections is given in table 3 and in figure 3, with the minimization of the absolute value of the maximal difference as the matching criterion. It is clear that, while being rather small for the central line (1/2, −1/2), these corrections are quite important for the satellite lines. Unfortunately, even for corrections of, say, 20%, the experiment will be completely unable to detect the change in the shape of the relaxation curve; figure 3 shows that by using time scaling the corresponding deviations can be reduced to less than 0.7% of the total variation of the signal, which is usually completely covered by noise.

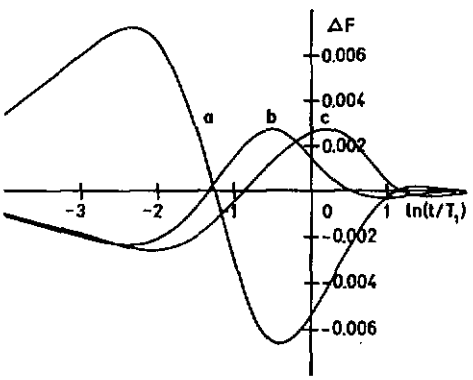


**Figure 3.** Time dependence of the difference $\Delta F$ between the real curve and the time-scaled 'standard' relaxation curve, corresponding to the $H_0 = 5.75$ T case of table 3 for the (*a*) low, (*b*) central and (*c*) high frequency lines. All curves are normalized to $F(t = 0) = 1$.

Note that in principle the above time-scaling procedure can be used to correct the data obtained by the formal use of the standard curves given in table 1. However, depending on the fit of the experimental data and the exact matching criterion used in the scaling, it is easy to introduce systematic errors in this correction. In fits it is always preferable to use the exact curve directly without further corrections.

We return to the discussion of the frequency independence of the relaxation rate (9), which enables us to define the single parameter $T_1$ describing multiexponential relaxation. We already mentioned that deviations from frequency independence are not likely to be encountered. Nevertheless, they are discussed here as the natural generalization of the previous analysis leading to the most general case of 'arbitrary' transition probabilities (which include quadrupole relaxation). The main point is that one is able to detect experimentally the possible deviations from the frequency-independent $T_1$ (and/or from magnetic relaxation); first we look for the possible differences between the theoretical and experimental form of the relaxation. Although this depends on the noise in the experiment, we already saw in figure 3 that there is a fair chance that the possible change in the form of the curve can be absorbed in the time-scaling factor and consequently in the false $T_1$ value. It is therefore necessary to check whether the same relaxation rate is obtained in measurements on different

**Table 2.** Magnetic field dependence of the (coefficients defining) relaxation curves $F(t/T_1) = \sum_{i=1}^{3} a_i \exp(-b_i t/T_1)$ corresponding to the plane copper resonance in $YBa_2Cu_3O_7$ for $H_0$ perpendicular to the symmetry axis, transition (3/2, 1/2), $\nu_Q = 31.48$ MHz and NSLRR anisotropy $R = 3.73$ [5]. The second column contains the reference in which the given value of $H_0$ has been used in the measurements.

| $H_0(T)$ | Ref. | $a_1$ | $b_1$ | $a_2$ | $b_2$ | $a_3$ | $b_3$ |
|---|---|---|---|---|---|---|---|
| 0.44 | [6] | 0.000 03 | 8.02 | 0.969 | 1.95 | 0.031 | 0.825 |
| 0.88 | [6] | 0.0010 | 7.52 | 0.898 | 2.33 | 0.101 | 0.869 |
| 2.2 | — | 0.069 | 6.21 | 0.747 | 3.13 | 0.184 | 0.953 |
| 5.75 | [9] | 0.264 | 5.98 | 0.586 | 3.07 | 0.151 | 0.991 |
| 8.1 | [5] | 0.304 | 5.99 | 0.559 | 3.04 | 0.137 | 0.995 |
| $\infty$ | | 0.4 | 6 | 0.5 | 3 | 0.1 | 1 |

NMR lines of the same spectrum [3, 8]. Note that 'looking' at each line, one finds its relaxation curve predominantly determined by the transition probability corresponding to this line. (This plausible statement can easily be supported numerically if we look at the changes in the relaxation curve when different transition probabilities are forced 'by hand' to deviate from the standard case of (10).) Any frequency dependence will thus be directly observable. Moreover, once the relaxation has been measured for all the lines, it is in principle possible to deduce exactly all the values $T_1(\omega_{mk})$ corresponding to each line, i.e. in this way one can directly measure the frequency dependence of NSLRR. The determination will be iterative, similar to the above discussed determination of $T_1$ using (13), where once again the starting values will be taken from the standard analysis. Of course, if (10) is valid for the chosen crystal axis, this procedure can be carried out independently for this direction. In principle, even the most general case based on (12) is solvable; however, this demands the simultaneous knowledge of relaxation for all the lines, for all the crystal axes. In the most general case we will actually determine all the transition probabilities irrespective of their values. Thus, even the restriction to magnetic relaxation (6) is no longer necessary. However, it is clear that this implies a rather demanding quantity of experimental information.

**Table 3.** Time-scaling coefficients $k$ which minimize the difference $\Delta F = [F(H_0, t/T_1) - F(H_0 = \infty, kt/T_1)]$ between the real curve (see table 2) and the time-scaled 'standard' relaxation curve (see table 1 for spin 3/2). The coefficients $k$ measure the error in the determination of $T_1$ when 'standard' curve is used instead of the real one.

| $H_0(T)$ | 5.75 | 8.1 |
|---|---|---|
| Reference | [9] | [5] |
| Low freq. satellite | 1.198 | 1.133 |
| Central line | 0.962 | 0.981 |
| High freq. satellite | 0.868 | 0.901 |

As regards the most general case, we recall that when different isotopes of the same nucleus are available, as e.g. for copper $^{63}Cu$ and $^{65}Cu$, the measurement of the ratio of NSLRR of two different isotopes can be compared to the ratio of squared nuclear gyromagnetic ratios or quadrupole moments in order to deduce the origin of nuclear relaxation, as has been done, e.g. in [6]. If this is not possible, (e.g. in the case

of $^{17}$O NMR) one should rely on the analysis of the relaxation curves for different lines of the same spectrum, as in the case where the possibility of frequency-dependent $T_1$ has been discussed.

## 4. Conclusion

For nuclear spins greater than 1/2 the quadrupole coupling splits the NMR line and makes the determination of characteristic tensors, i.e. the MHS, EFG and NSLRR tensors, more difficult. Orthorhombic symmetry and the local symmetry $mm2$ can considerably simplify this determination; in the coordinate system of crystal axes the tensors are then diagonal and we show that the choice of orientation with the external field $\boldsymbol{H}_0$ parallel to one of the crystal axes is particularly advantageous in the measurements. In this case only one complete spectrum is needed for the full determination of the EFG tensor.

In the measurements of NSLRR ($T_1^{-1}$) the existence of several NMR lines in the spectrum of one nucleus will imply multiexponential relaxation. In appendix A a general procedure is given which predicts the form of relaxation for any set of transition probabilities and initial conditions. In fact, one would like to have the 'inverse procedure' which would calculate the transition probabilities from the experimentally determined form of relaxation. In principle, if the relaxation form is known for all the NMR lines, one can determine the transition probabilities using the procedure as given in appendix A in an iteration, until the self-consistent solution is found. We are primarily interested in the case where only one parameter determines the transition probabilities: for the relaxation of magnetic origin this parameter is defined in the trivial case of spin 1/2 where the relaxation is single-exponential with the time constant $T_1$ measuring the transverse fluctuations of magnetic field (at the NMR frequency) according to (9) and (7). For spins greater than 1/2 the same parameter is still the only one which determines the transition probabilities according to (10), if the Zeeman spin states are left (almost) unperturbed by the quadrupole coupling, and if $T_1$ does not depend on the frequency of the transition. In this case the simple application of the procedure given in appendix A gives 'standard' multiexponential relaxation curves (which depend only on the spin value and on the chosen transition—examples are given in table 1) and one measurement of relaxation (on any one of the lines) is sufficient for the determination of $T_1$ for the chosen orientation of $\boldsymbol{H}_0$.

However, if the Zeeman spin states are significantly mixed by the quadrupole coupling, while the frequency independence of $T_1$ parameters (9), (7) is still valid, transition probabilities are defined by three parameters which can be reduced to the definitions of $T_1$ (9), (7) for three directions of crystal axes $a$, $b$ and $c$. For the determination of these, one needs one relaxation measurement for each of the three orientations of the sample. There are no more 'standard' relaxation curves, as they are specific to each case and have to be determined self-consistently for all three orientations (e.g. see table 2). In this paper we were especially interested in considering how a small quadrupole perturbation of Zeeman levels is reflected in the corresponding deviation from the 'standard' relaxation curves. We found that corrections are needed as soon as the Zeeman energy $\hbar\gamma_n H_0$ is only a few times greater than the quadrupole coupling $h\nu_Q$. In this case only one iteration is usually sufficient in the iterative determination of $T_1(a, b, c)$. Finally, if we allow for the frequency dependence of $T_1$, we have achieved the above-mentioned case where all

the transition probabilities are unknown and one has to measure relaxation on all the lines of the spectrum.

For the analysis of multiexponential relaxation to be valid, it is of course imperative to have well defined initial conditions, as they also directly determine the form of relaxation (see (A12) in appendix A). The choice of excitation discussed in this paper corresponds to the standard $T_1$ pulse sequence $\pi$–$t$–$\pi/2$–$\tau$–$\pi$ where only a single line is excited by the pulse (sequence) which is very short on the time scale defined by the fastest-relaxing exponential in the relaxation.

Finally, as regards the numerical analysis needed in the definition of relaxation curves, our choice of Hamiltonian (2) ensures that the arithmetic is real, while the matrix formulation of the procedure given in appendix A allows its easy conversion to a computer program. For example, in the course of this work 'Mathematica' programming package has been used, in which all the formulae we use have almost direct equivalents in the program (up to the syntax of the language). The same 'Mathematica' program was used to obtain the exact solutions (i.e. solutions given in rational numbers) for the 'standard' curves, as those given in table 1, as well as the 'ordinary' numerical results, as those given in table 2.

## Appendix A

We suppose that the spin–spin interactions ensure that the population of energy levels of each spin can be treated statistically. The time dependence of the average population $n_i$ of the $i$th energy level is then described by the linear rate equation

$$\mathrm{d}n_i/\mathrm{d}t = \sum_{j=1}^{N}{}' (W_{ij}n_j - W_{ji}n_i) \qquad i = 1, 2, \ldots, N = 2I + 1 \quad \text{(A1)}$$

where $W_{ij}$ is the probability of transition from level $j$ to level $i$, and the prime on $\sum$ denotes the absence of $i = j$ terms. For convenience, (A1) can be cast in the (obvious) matrix notation:

$$\mathrm{d}\boldsymbol{n}/\mathrm{d}t = \mathbf{U}\boldsymbol{n} \qquad \text{(A2)}$$

where

$$U_{ij} = \begin{cases} W_{ij} & \text{for i} \neq j \\ -\sum_k{}' W_{ki} & \text{for i} = j. \end{cases} \qquad \text{(A3)}$$

As the rate equation (A1) respects the normalization condition

$$\sum_{i=1}^{N} n_i = 1 \qquad \text{(A4)}$$

the variables $n_i$ are not independent. As a convenient set of independent variables we choose the difference of populations of neighbouring energy levels

$$\Delta n_i = n_i - n_{i+1} \qquad i = 1, 2, \ldots, N - 1 = 2I \qquad \text{(A5)}$$

which is directly proportional to the NMR signal from the corresponding transition $(i+1, i)$. In order to transform (A2) to these new variables, we define a convenient transformation matrix **D** [14]:

$$D_{ij} = \begin{cases} \delta_{ij} - \delta_{i+1,j} & \text{for } i \leqslant N-1 \\ 1 & \text{for } i = N \end{cases} \tag{A6}$$

where $\delta_{ij}$ is the Kronecker delta. Applying the **D** matrix to (A2) and using the normalization condition (A4) we obtain:

$$\mathrm{d}\Delta\boldsymbol{n}/\mathrm{d}t = -\mathbf{A}\Delta\boldsymbol{n} + \boldsymbol{b} \tag{A7}$$

where for $i, j = 1, 2, \ldots, N-1 = 2I$,

$$-A_{ij} = (\mathbf{DUD}^{-1})_{ij} \tag{A8}$$

and

$$b_i = (\mathbf{DUD}^{-1})_{iN} = \frac{1}{N}\sum_{k=1}^{N}[(W_{ik} - W_{ki}) - (W_{i+1,k} - W_{k,i+1})]. \tag{A9}$$

(From definitions (A3) and (A6) we can show that the last row of the $\mathbf{DUD}^{-1}$ matrix is equal to zero: $(\mathbf{DUD}^{-1})_{Ni} = 0$, for $i \leqslant N$.) From (A7) and (A9) we see that the equilibrium occupation difference,

$$\Delta\boldsymbol{n}(\infty) = \mathbf{A}^{-1}\boldsymbol{b} \tag{A10}$$

is proportional to the asymmetry of the transition probabilities. The approach to the equilibrium is governed by the linear homogeneous matrix equation

$$\mathrm{d}[\Delta\boldsymbol{n}(t) - \Delta\boldsymbol{n}(\infty)]/\mathrm{d}t = -\mathbf{A}[\Delta\boldsymbol{n}(t) - \Delta\boldsymbol{n}(\infty)]. \tag{A11}$$

The solution of (A11) can be written as

$$\Delta n_i(t) = \Delta n_i(\infty) + \sum_{j,k} C_{i,j}\exp(-\lambda_j t)C^{-1}_{j,k}[\Delta n_k(0) - \Delta n_k(\infty)] \tag{A12}$$

where **C** is the matrix made of the eigenvectors of the matrix **A**; the $i$th column of the matrix **C** is an eigenvector of the matrix **A** which corresponds to the eigenvalue $\lambda_i$. The expression in the brackets on the right-hand side of the equation is determined by the initial conditions. Note that (A3, A6, A8, A12) define a procedure which can be directly converted to a computer program. Note that the transition probabilities contain an unknown prefactor $T_1^{-1}$, and the time variable has to be changed to $t/T_1$ in order to leave only the fixed numbers in the procedure.

**Acknowledgment**

The author is deeply grateful to Drs C Berthier, Y Berthier, P Ségransan and P Butaud—members of the solid state NMR group in Laboratoire de Spectrométrie Physique (UA 08 CNRS), Université Joseph-Fourier Grenoble I, where the experimental basis for this work has been carried out.

## References

[1] Slichter C P 1990 *Principles of Magnetic Resonance* 3rd edn (Berlin: Springer)
[2] *Proc. M²HTSC Conf. (Lake Kanazawa, 1991); Physica* C 185–9
[3] Pennington C H, Durand D J, Zax D B, Slichter C P, Rice J P and Ginsberg D M 1988 *Phys. Rev.* B **37** 7944
Pennington C H, Durand D J, Slichter C P, Rice J P, Bukowski E D and Ginsberg D M 1989 *Phys. Rev.* B **39** 2902
[4] Horvatić M, Ségransan P, Berthier C, Berthier Y, Butaud P, Henry J Y, Couach M and Chaminade J P 1989 *Phys. Rev.* B **39** 7332
[5] Barrett S E, Martindale J A, Durand D J, Pennington C H, Slichter C P, Friedmann T A, Rice J P and Ginsberg D M 1991 *Phys. Rev. Lett.* **66** 108
[6] Takigawa M, Smith J L and Hults W L 1991 *Phys. Rev.* B **44** 7764
[7] Takigawa M, Hammel P C, Heffner R H, Fisk Z, Ott K C and Tompson J D 1989 *Phys. Rev. Lett.* **63** 1865
Horvatić M, Berthier Y, Butaud P, Kitaoka Y, Ségransan P, Berthier C, Katayama-Yoshida H, Okabe Y and Takahashi T 1989 *Physica* C **159** 689
Hammel P C, Takigawa M, Heffner R H, Fisk Z and Ott K C 1989 *Phys. Rev. Lett.* **63** 1992
[8] Butaud P, Horvatić M, Berthier Y, Ségransan P, Kitaoka Y, Berthier C and Katayama-Yoshida H 1990 *Physica* C **166** 301
[9] Horvatić M, Berthier C, Berthier Y, Butaud P, Clark W G, Gillet J A, Ségransan P and Henry J Y 1991 *Physica* C **185–9** 1139; 1992 *Phys. Rev. Lett.* submitted
[10] Horvatić M 1991 *Thesis* Zagreb University, unpublished
[11] Andrew E R and Tunstall D P 1961 *Proc. R. Phys. Soc.* **78** 1
[12] Narath A 1967 *Phys. Rev.* **162** 320
[13] Chepin J and Ross Jr J R 1991 *J. Phys.: Condens. Matter* **3** 8103
[14] Robin J M 1990 Private communication